Environ Sci Pollut Res (2014) 21:11418–11432
DOI 10.1007/s11356-014-3078-2

RESEARCH ARTICLE

Seasonal trends, meteorological impacts, and associated health risks with atmospheric concentrations of gaseous pollutants at an Indian coastal city

Parth Sarathi Mahapatra · Sipra Panda · P. P. Walvekar · R. Kumar · Trupti Das · B. R. Gurjar

Received: 16 March 2014 / Accepted: 20 May 2014 / Published online: 7 June 2014

Abstract This study presents surface ozone (O_3) and carbon monoxide (CO) measurements conducted at Bhubaneswar from December 2010 to November 2012 and attempts for the very first time a health risk assessment of the atmospheric trace gases. Seasonal variation in average 24 h O_3 and CO shows a distinct winter (December to February) maxima of 38.98±9.32 and 604.51±145.91 ppbv, respectively. O_3 and CO characteristics and their distribution were studied in the form of seasonal/diurnal variations, air flow patterns, inversion conditions, and meteorological parameters. The observed winter high is likely due to higher regional emissions, the presence of a shallower boundary layer, and long-range transport of pollutants from the Indo-Gangetic Plain (IGP). Large differences between daytime and nighttime O_3 values during winter compared to other seasons suggest that photochemistry is much more active on this site during winter. O_3 and CO observations are classified in continental and marine air masses, and continental influence is estimated to increase O_3 and CO by up to 20 and 120 ppbv, respectively. Correlation studies between O_3 and CO in various seasons indicated the role of CO as one of the O_3 precursors. Health risk estimates predict 48 cases of total premature mortality in adults due to ambient tropospheric O_3 during the study period. Comparatively low CO concentrations at the site do not lead to any health effects even during winter. This study highlights the possible health risks associated with O_3 and CO pollution in Bhubaneswar, but these results are derived from point measurements and should be complemented either with regional scale observations or chemical transport models for use in design of mitigation policies.

Keywords O_3 winter maxima · Meteorological analysis · Transport pathways · Correlation analysis · Columnar NO_2 · Health risk

Responsible editor: Gerhard Lammel

P. S. Mahapatra · S. Panda · T. Das (✉)
Environment and Sustainability Department, CSIR-Institute of Minerals and Materials Technology, Bhubaneswar, Odisha 751013, India
e-mail: trupti.sreyas@gmail.com

T. Das
e-mail: truptidas@immt.res.in

P. P. Walvekar · B. R. Gurjar
Department of Civil Engineering, Indian Institute of Technology Roorkee, Roorkee, India

R. Kumar
Atmospheric Chemistry Division, National Center for Atmospheric Research, Boulder, CO, USA

Introduction

Development in urban/industrial sectors and agricultural expansion around the world has led to a rapid increase in emissions of anthropogenic pollutants and has consequently resulted in degradation of air quality. Tropospheric ozone (O_3) is a key air pollutant as high concentrations of O_3 near the surface can lead to adverse health effects (Desqueyroux et al. 2002) and damage vegetation (e.g., Mauzerall and Wang 2001). It is estimated that the increase in tropospheric O_3 due to human activities since 1850 might be responsible for 470,000 premature mortalities globally every year (Silva et al. 2013). Study of Lelieveld et al. (2013) has also placed India to be the second country globally for respiratory mortality by O_3 pollution. O_3 is also a potent greenhouse gas and contributes to global warming by absorbing infrared radiation at 9.6 μm. Considered to be a major precursor of hydroxyl (OH) radical, O_3 is a primary oxidizing agent and controls the lifetime of many toxic species in the atmosphere (Lin et al. 2011). Tropospheric O_3, a secondary pollutant, is produced mainly

by a complex set of reactions among its precursors (carbon monoxide (CO) and hydrocarbons) in the presence of sunlight (Crutzen 1973; Levine 1996; Kalita and Bhuyan 2011; Sikder et al. 2011) and nitrogen oxides (NOx). The influx from the stratosphere also contributes to tropospheric O_3 concentrations. However, this contribution (23 %) is estimated to be lower than the photochemical production (77 %) (Sudo and Akimoto 2007).

CO is also a key air pollutant owing to its ability to affect human health (Aubard and Magne 2000). The importance of CO from the perspective of atmospheric chemistry is quite relevant as it plays a crucial role in tropospheric O_3 formation (Fishman and Seller 1983) and affects tropospheric oxidation capacity by removing OH radical. It is estimated that 60 % of annual global CO is generated from anthropogenic activities (including combustion of fossil fuel and agriculture waste burning) and the rest through natural sources such as forest fires (Khalil and Rasmussen 1990; Olivier et al. 1999) and oxidation of hydrocarbons. Due to growing population and associated increase in various human activities related to industrial, transportation, and power generation sectors, anthropogenic emissions of trace gases and aerosols are increasing rapidly in South Asia (Ohara et al. 2007; Kurokawa et al. 2013). In addition, residential bio-fuel and biomass burning have also been suggested as a significant source of O_3 precursors and carbon-containing aerosols (Lawrence and Lelieveld 2010). These rising emissions can potentially affect the distribution of tropospheric O_3, and therefore, measurements of O_3 and precursor trace gases are highly essential in this region.

In view of the above, measurements of surface O_3 and precursor gases have been conducted at many stations in India to derive information about the diurnal/seasonal variations and processes controlling surface O_3 (e.g., Lal et al. 2000; Naja and Lal 2002; Naja et al. 2003; Beig et al. 2007; Reddy et al. 2008; Purkait et al. 2009; Kumar et al. 2010; Ojha et al. 2012). Earlier studies of surface O_3 in the Indian region focused mainly in western and southern parts of India, and first observations of surface O_3 from eastern India have been reported very recently (Purkait et al. 2009; Mahapatra et al. 2012). However, both these studies have qualitatively discussed the possible processes controlling surface O_3 at the respective observation sites. In this study, we aim at advancing our understanding of chemical characteristics of air masses in eastern India by complimenting surface O_3 observations presented by Mahapatra et al. (2012) with CO observations. Wind direction measurements are also used to estimate the influence of continental and marine air masses on O_3 and CO levels, along with O_3–CO relationships at Bhubaneswar. In addition, we have estimated the health effects in terms of total, respiratory, and cardiovascular premature mortality for adults (age 15–60 years) associated with ambient air concentrations of CO and O_3 during the study period of December 2010 to November 2012. Numerous epidemiological studies in both developing and developed countries have proved the linkages of increased ambient pollutant levels to elevated human health risks (Pope et al. 2002; HEI 2004, 2010, 2011; Cao et al. 2011; Patankar and Trivedi 2011; Lelieveld et al. 2013). In a global study, it was estimated that 0.8 million annual premature deaths and loss of 6.4 million life years occur as a result of global air pollution, and two third of these account for in Asian developing countries (Cohen 2005) suggesting the importance of carrying out such studies. The manuscript provides a description of observation site, general meteorology prevailing at this site, measurement techniques, and methodology in "Materials and methods." The results of this study are discussed in "Results and discussions," and conclusions drawn are presented in "Conclusion."

Materials and methods

Site description

The observations of trace gases and meteorological parameters used in this study are made at CSIR-IMMT, Bhubaneswar (20° 30′ N and 85° 83′ E), which is the capital city of an eastern coastal state named Odisha, located in tropical India. The city has a population of 837,737 (http://www.census2011.co.in/census/city/270-bhubaneswar.html), situated at an altitude of 45 m above sea level and at a distance of ~60 km west of the northern Bay of Bengal. Bhubaneswar is undergoing rapid development and is continuously expanding along the outskirts, due to the establishment of a few globally known organizations and its connectivity to major cities. The major industrial belt (cement, thermal power station, mining activities, and metallurgical plants such as sponge iron) of Odisha lies in the northwest direction of the site, a missile testing site at Chandbali is also located northeast direction, and few major sea ports and fertilizer plants lie to the eastern part of the site. These industries are located at an approximate radius of 200 km from the site and could be potential sources of trace gases and aerosols in the atmosphere. Consequently, the city has been experiencing deterioration of air quality and reduced visibility especially during winters. The nearest major metropolitan city is Kolkata, due northeast. The present sampling site is approximately 1.5 km away from National Highway-5 dominated by vehicular emissions.

General meteorology

The site experiences distinct weather conditions throughout the year, namely, pre-monsoon (March, April, May (MAM)), monsoon (June, July, August (JJA)), post-monsoon (September, October, November (SON)), and winter (December, January, February (DJF)). The variations in

monthly minimum and maximum temperature, average relative humidity, and total rainfall from December 2010 to November 2012 are shown in Fig. 1. The site receives maximum solar radiation annually during the pre-monsoon followed by post-monsoon, winter, and a minimum during monsoon. Temperature shows a distinct seasonal cycle with a minimum of about 10 °C during winter and a maximum of 40°–45 °C in pre-monsoon season. The relative humidity (RH) is always more than 50 % in Bhubaneswar because of its proximity to the Bay of Bengal and exceeds 80 % during June–September indicating the arrival and prevalence of Indian summer monsoon during these months. RH again decreases to about 50–60 % during post-monsoon as the monsoon retreats. Total rainfall at the site shows a dramatic increase during the monsoon months, and the average rainfall during June–August is estimated as 220 mm per month. The seasonal variation in solar radiation (not shown) is characterized by a pre-monsoon season maximum and a monsoon minimum. During winter season, wind parcels arrived from the Indo-Gangetic Plain (IGP) and parts of western India toward Bhubaneswar at a uniform wind speed (<3 m/s). In the pre-monsoon, season winds come from the Bay of Bengal and from the other scattered directions. During monsoon, winds show a typical southwestern origin, while the post-monsoon season bears a shift from southwest to northerly scattered directions. These explanations have been discussed elaborately in Mahapatra et al. (2012).

Measurement techniques

Continuous measurements of near surface O_3 and CO are being made in Bhubaneswar using online analyzers for O_3 (Thermo Scientific Model 49i) and CO (HORIBA APMA-370). O_3 measurements are based on the principle of UV-photometric absorption at 254 nm, while CO measurements are based on the cross modulation type non-dispersive infrared analysis. Both the analyzers are placed on the roof of the Council of Scientific and Industrial Research's (CSIR's) Institute of Minerals and Materials Technology (IMMT) and aspirate ambient air through Teflon tubes from a height of about 20 m above the ground level with a flow rate of 1.5 L min^{-1}. The minimum detection limit of the O_3 analyzer is 1.0 ppbv with a 20-s response time, and the data is averaged at every 15-min interval. The O_3 analyzer is calibrated at regular intervals with the help of internal ozonator (O_3 generator) and zero gas to maintain the accuracy of the readings (Mahapatra et al. 2012). The minimum detection limit of the CO analyzer is 0.05 ppm for ranges of≤10 ppm with response time of 60 s and the data are averaged at every 30 min interval. To maintain the accuracy of CO observations, CO analyzer is regularly calibrated using National Institute of Standards and Technology (NIST) traceable standard gas through the help of a dynamic gas calibrator (Thermo Scientific 146i). The analyzers are connected to a personal computer, and the data are downloaded at regular intervals, using suitable software, for further analysis and interpretation.

Meteorological parameters at this site are measured using an automatic weather station (AWS) RainWise, Inc (CC-3000) and cross checked with the data from the Indian Meteorological Department, Bhubaneswar. Both the data sets show a strong positive relationship (Tmax (R^2=0.99); Tmin (R^2=0.96); RH (R^2=0.77); mean sea level pressure (R^2=0.85). Solar flux (direct and diffused) is measured through a pyranometer (Campbell Scientific—CR 850) within the wavelength range of 0.285 to 2.8 μm. AWS collects data every 15 min and runs continuously throughout the year. These 15-min data are averaged for a day and then for a month to determine the monthly average.

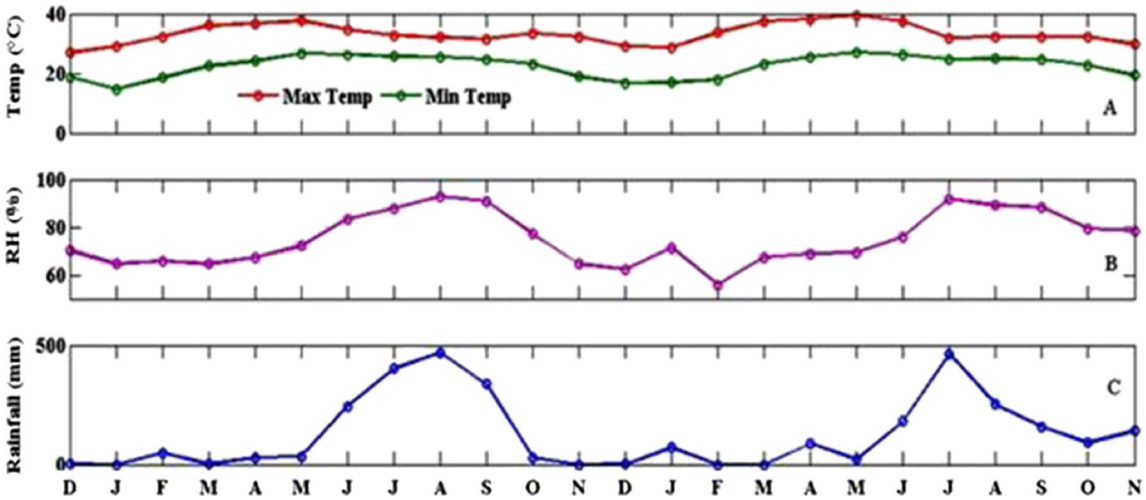

Fig. 1 Monthly average **a** minimum and maximum temperature (°C), **b** % RH, and **c** total rainfall (mm) in each month during December 2010 to November 2012

Health risks estimation methodology

The number or cases of health effects in terms of mortality or morbidity are estimated by using (1) a concentration response function (CRF), i.e., change in the number of excess cases per unit change in concentration of the pollutant per capita or relative risk (RR); (2) incidence rate of mortality or morbidity; (3) change in ambient air concentration; and (4) exposed population. The health effect of ambient air pollutant concentrations in terms of mortality depends upon a functional form of the relationship. If the functional form of CRF is log-linear, excess mortality can be estimated by using a health impact function given in Eq. (1) (Penney et al. 2009; Lelieveld et al. 2013).

$$\Delta H = \left(e^{\beta \times \Delta C} - 1\right) \times I \times P \quad (1)$$

where,

ΔH	The number of several health effects (mortality/morbidity)
β	Concentration response function
ΔC	Change in ambient air concentration
P	Exposed population
I	Incidence rate of mortality

The change in the number of excess cases per unit change in concentration is termed as CRF (β). These are extracted from epidemiological studies conducted in the study area context (Table 1). The change in air quality (ΔC) under consideration is generally taken as a difference between ambient air pollutant concentration and concerned national ambient air quality standards (NAAQS) or World Health Organization (WHO) air quality guidelines. The exposed population (P) can be the entire population or sensitive subgroups like children or elderly persons according to the targeted population and related health impacts. The incidence rate of mortality is the measure of probability of death before reaching his 60th birthday (in case of adult, i.e., age group 15–59 years) per 1,000 population per year in a hypothetical cohort of 100,000 people.

According to Lelieveld et al. (2013), relative risk associated with change in ambient concentration of pollutant is given by Eq. (2).

$$\mathrm{RR} = e^{\beta \times \Delta C} \quad (2)$$

where, RR=changed relative risk of the health effect.

If the functional form of CRF has a linear relationship, Eqs. (3), (4), and (5) are used for estimating the health impacts associated with ambient air pollution depending upon availability of CRFs (Ostro 1994; Lvovsky et al. 2000; Guttikunda and Goel 2012) or relative risks (Gurjar et al. 2010; Cropper et al. 2012).

$$\Delta H = \beta \times I \times \Delta C \times P \quad (3)$$

$$\mathrm{APF} = \frac{\mathrm{RR}-1}{\mathrm{RR}} \quad (4)$$

$$\Delta H = (\mathrm{RR}-1) \times I \times (1-\mathrm{APF}) \times P \quad (5)$$

Input parameters

In this study, the health effects are estimated associated with increased ambient CO and O_3 pollution levels compared to WHO guidelines of 10,000 and 100 μg/m^3, respectively (WHO 2006). The mortality, health endpoints are most extensively taken into account for health risk evaluation studies because of the fact that death is the most clearly defined health endpoint (Kandlikar and Ramachandran 2000). Therefore, we have estimated the health effects for adults (age 15–60 years) in terms of total, respiratory, and cardiovascular premature mortality due to exposure to the above-mentioned pollutants.

To estimate the human health effects most accurately, one should conduct an epidemiological study to link the air pollutant exposures to increased human health endpoints. However, owing to financial, time, and professional constraints, it becomes essential to transfer the CRFs (β) from

Table 1 CRFs; concentration response functions (change in health effects per capita per 1 μg/m^3 change in CO and O_3)

	Total mortality			Respiratory mortality			Cardiovascular mortality		
	Lower limit	Average	Higher limit	Lower limit	Average	Higher limit	Lower limit	Average	Higher limit
CO	0.00011	0.00034	0.00057	–	–	–	–	–	–
O_3	−0.00016	0.00007	0.0003	0.0003	0.00073	0.000116	−0.00029	0.00012	0.00054

one study to another. In this study, we used the CRFs in a range within which it is likely to fall along with the central estimate so as to reduce uncertainty due to transfer of CRFs. The CRFs are adopted from Atkinson et al. (2011) who conducted a meta-analysis of 115 global epidemiological studies.

The number of premature deaths per unit age group population in a year is well described by incidence rate (*I*) for premature mortality. The incidence rate of mortality is the measure of probability of premature death between 15 and 60 years of age (this study takes into account adults) per 1,000 population per year in a hypothetical cohort of 100,000 people. The types of deceases are classified according to ICD-10 (International classification system for diseases—version 10) given by the World Health Organization (WHO). The ICD-10 codes used for all causes, cardiovascular, respiratory, and lung cancer, of premature mortality are A00–R99, I00–I99, J00–J99, and C33–C34, respectively. Total incidence rate (number of deaths per unit population) of premature mortality for this study domain is adapted from (RGI 2012a) 201 per 1,000 people and adjusted for disease-specific premature mortality (i.e., number of disease-specific deaths per unit population) such as respiratory and cardiovascular premature mortality of 6.8 and 23.3 %, respectively (RGI 2012b). The population for the study domain is extracted from the 2011 census, and it is observed that 67.1 % of the population is within the age group of 15–59 years (RGI 2012a). Furthermore, based on a study conducted by Guttikunda and Goel (2012), 55 % of the population is assumed to be vulnerable to ambient (outdoor) exposure.

Results and discussions

Seasonal variation in O_3 and CO

The seasonal variation in near surface O_3 and CO measured at Bhubaneswar during December 2010–November 2012 is discussed in this section. The results presented here are an extension of Mahapatra et al. (2012a), who qualitatively discussed the processes controlling seasonal variations in surface O_3 at Bhubaneswar during December 2009 to January 2011. The variations in monthly average O_3 and CO for daytime (11:00 A.M.–4:00 P.M.), nighttime (01:00 A.M.–03:00 A.M.), and 24 h average data at Bhubaneswar during December 2010 to November 2012 are shown in Fig. 2. Monthly average values are calculated from daily averages estimated using 15-min data for O_3 and 30-min data for CO. O_3 and CO measurements during March 2011–April 2011 are unavailable as the instruments were shut down to avoid contamination in observations due to the ongoing construction work at the measurement site, and O_3 data are again unavailable during April 2012–May 2012 due to a technical snag in the analyzer.

Monthly average O_3 values at Bhubaneswar are highest during winter, decrease through the pre-monsoon season to attain lowest values during August–Septemeber, and again increase during October–November. Daily 24-h average of O_3 values during winter (DJF), pre-monsoon (MAM), monsoon (JJA), and post-monsoon (SON) seasons are estimated at 39±9, 33±10, 29±6, and 28±8 ppbv, respectively. More or less similar concentrations of surface O_3 during monsoon and post-monsoon seasons were likely due to the effect of extended monsoon even during the month of September (Fig. 1) and retreating monsoon during October and November 2012. This could have lead to a lower surface O_3 concentration during post-monsoon. The daytime monthly average values of O_3 showed a similar seasonal trend during both the years (2011, 2012) with a maximum concentration during winter followed by pre-monsoon, post-monsoon, and a minimum during monsoon. The nighttime O_3 monthly average values also showed a similar trend of a winter high and monsoon low during the year 2011, whereas during 2012, the monthly variations in nighttime O_3 were different. Maximum nighttime O_3 concentration was detected in monsoon that was followed by winter, post-monsoon, and pre-monsoon. This night-time maximum O_3 values during monsoon 2012 were due to lesser rain events during June 2012 accompanied with higher temperature conditions (Fig. 1) that could have created a congenial environment for higher O_3 production during June 2012 ultimately leading to a higher average O_3 value during monsoon 2012. The daytime and nighttime periods investigated in this study can be considered as the representative of maximum and minimum photochemical activity respectively. Hence, the difference between daytime and nighttime O_3 values can be considered as "photochemical O_3 build-up" at this site. Seasonal photochemical build up shows good variability with as high as 32.43 ppbv during winters followed by 25.91 ppbv during pre-monsoon, 20.21 ppbv in post-monsoon, and 8.01 ppbv during monsoon. The diurnal variation of the solar flux (Fig. 6) is observed to influence the O_3 build up as the incoming radiation was maximum during pre-monsoon, followed by winter, post-monsoon, and was lowest during monsoon. Therefore, O_3 buildup was also lowest during monsoon with a subsequent increase during post-monsoon. The winter and pre-monsoon build up at Bhubaneswar can be comparable to that of Pantnagar having values as high as 32–41 ppbv during spring and autumn and lowest during monsoon (Ojha et al. 2012).

CO values at Bhubaneswar were also detected to be highest during winter, and lowest values were observed during monsoon season. Average CO values during winter (DJF), pre-monsoon (MAM), monsoon (JJA), and post-monsoon (SON) seasons are estimated as 604±146, 262±54, 251±58, and 430±115 ppbv, respectively. The anthropogenic and biomass-

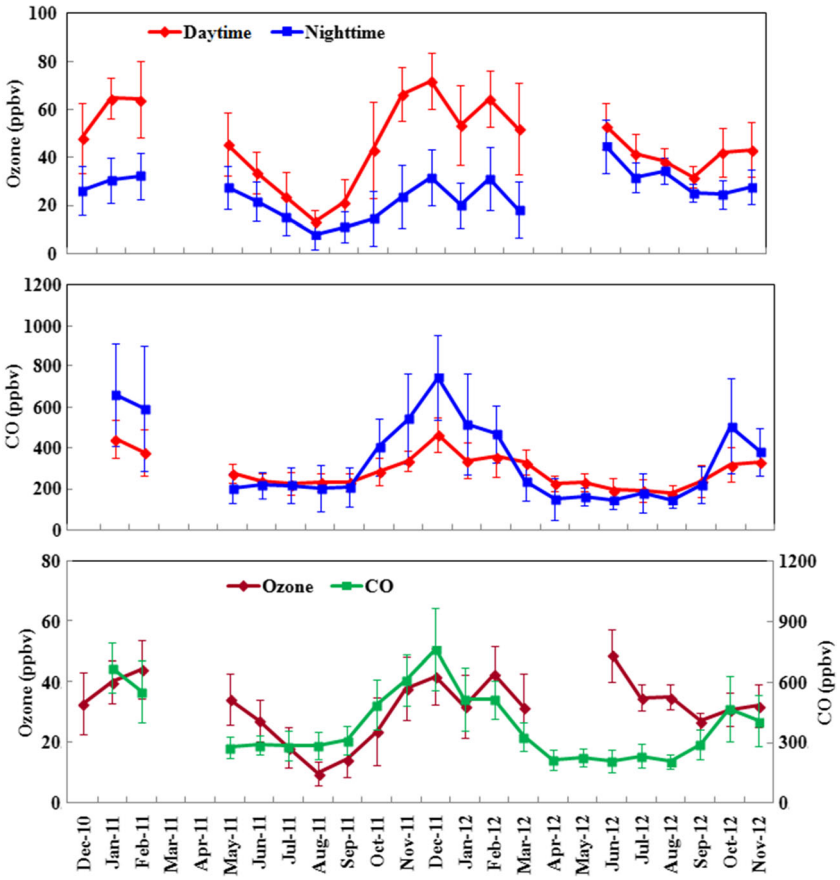

Fig. 2 Monthly average daytime, nighttime, and 24 h concentration of O_3 and CO during December 2010 to November 2012

burning emissions of CO from MACCity emission inventory (Granier et al. 2011) are analyzed to understand the role of regional emissions in controlling seasonal variations of CO at Bhubaneswar. MACCity emission inventory is an extension of the Atmospheric Chemistry and Climate Model Intercomparison Project (ACCMIP), a historical emissions project, and was developed as a part of two projects funded by the European Union, namely, Monitoring Atmospheric Composition and Climate (MAAC) and CityZen. The dataset was created for each compound and each sector to provide yearly emissions for the years 1960–2010 based on the emissions provided by ACCMIP and Representative Concentrations Pathways (RCP 8.5) datasets. CO is emitted by biogenic sources also, but their contribution to CO loadings in this region is very small (Kumar et al., 2013). Seasonal variations in anthropogenic and biomass-burning CO emissions over a geographical region (18°–26° N, 80°–90° E) around Bhubaneswar are shown in Fig. 3. It should be noted that anthropogenic emissions are representative of the year 2011, while biomass-burning emissions of CO are representative of the year 2008 as biomass-burning emissions for later years are not available from MACCity emission inventory. However, analysis of fire locations retrieved by Moderate Resolution Imaging Spectroradiometer (MODIS) (https://firms.modaps.eosdis.nasa.gov/firemap/) showed that fires during 2011 were not much different from those in 2008 (Fig. 4). Anthropogenic emissions in this region are higher by 1–4 orders of magnitude than the biomass-burning emissions and show seasonal variations very similar to the observed CO mixing ratios at Bhubaneswar. Biomass-burning emissions are highest during the pre-monsoon season but are not strong enough to alter the seasonality of anthropogenic

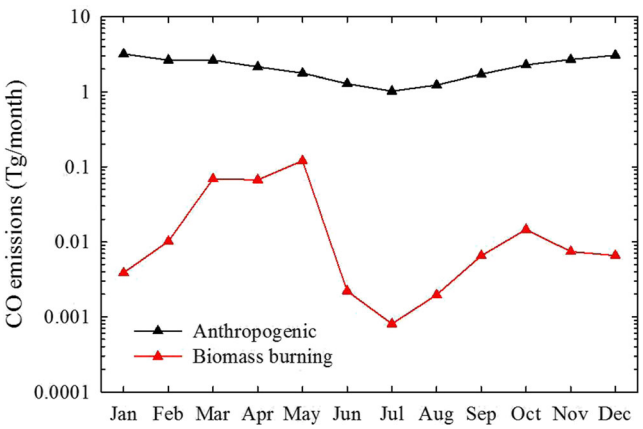

Fig. 3 Seasonal variation in anthropogenic and biomass-burning CO emissions over a geographical region (18°–26° N, 80°–90° E) around Bhubaneswar

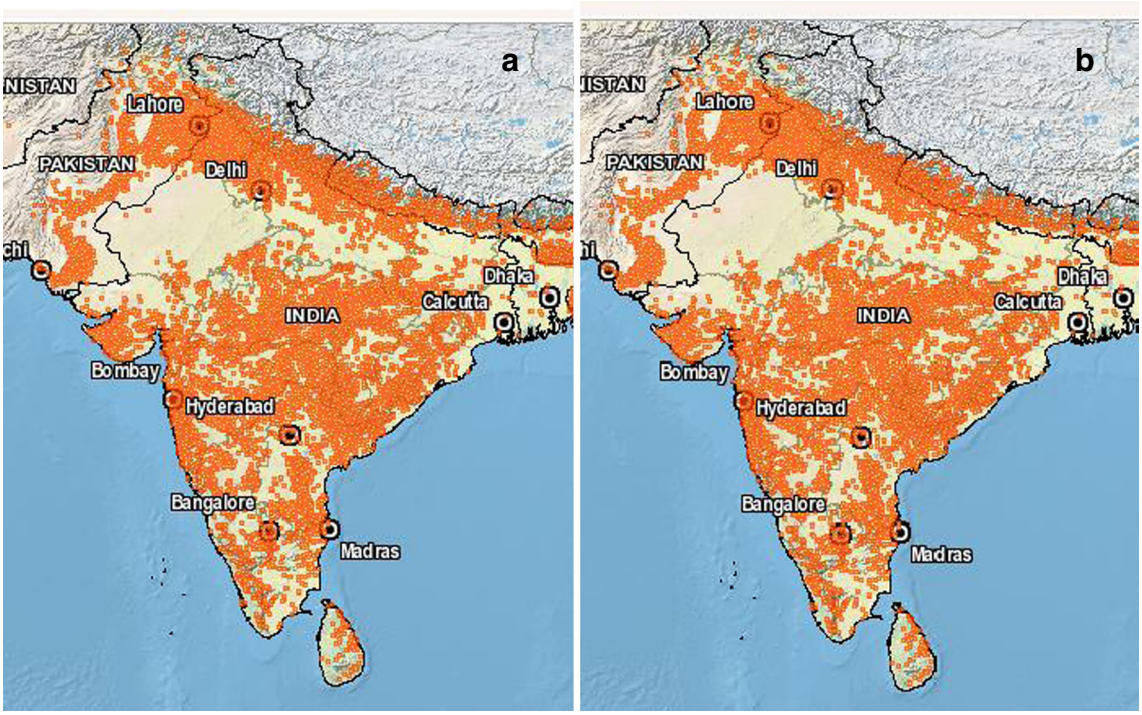

Fig. 4 Spatial distribution of fire counts over India during **a** 2008 (*left panel*) and **b** 2011 (*right panel*)

CO emissions. In addition to regional emissions, long-range transport of pollutants might also have some contribution to winter high in both O_3 and CO at Bhubaneswar as discussed in detail by Mahapatra et al. (2012a).

To put our observations into a national context, we compared our measurements with those available at various locations in India (Table 2). It is interesting to note that most of the sites (e.g., Kannur, Gadanki, Ahmedabad, Pune, Mt Abu, Trivandrum, Anantapur) due south of the Indo-Gangetic Plain also show highest O_3 values during winter and early pre-monsoon season, while the sites located within (Delhi, Pantnagar, Agra, Varanasi) or due north (Nainital) of the Indo-Gangetic Plain show highest O_3 values during pre-monsoon to early monsoon season. This indicates large spatial variability in surface O_3 distribution and diversity of regional O_3 sources in India. Diurnal CO concentration was also observed to be highest during winters (609±169.67 ppb) followed by post-monsoon (437.42± 133.60 ppb), pre-monsoon (265±60.29 ppb), and was lowest during monsoon (258.14±70.86 ppb).

Classification of O_3 and CO based on transport pathways

The changes in wind patterns can potentially affect the levels of trace gases at any site. Mahapatra et al. (2012a) used back-air trajectory calculations to discuss qualitatively the role of meteorology in seasonal variation of O_3 at Bhubaneswar. In this study, we use wind direction measurements to quantify the impact of changes in wind patterns on the levels of O_3 and CO at Bhubaneswar. For this, daytime O_3 and CO observations are classified into continental-polluted and marine air mass using wind direction measurements. All observations corresponding to wind direction in the quadrants 0–90, 181–270, and 271–360 are considered in the continental-polluted air mass group, and those in the quadrant 90–180 are included in the marine air mass group. However, back-air trajectory analysis showed that air masses arriving at Bhubaneswar during monsoon season originate from the oceanic regions of the Bay of Bengal, the Arabian Sea, and the Indian Ocean, but those originating in the Arabian Sea pass over the continental land mass before arriving at the site (Mahapatra et al. 2012). Thus, for monsoon season, all observations corresponding to wind direction in the quadrants 181–270 and 271–360 are considered in the continental-polluted group, and those in quadrants 0–90 and 91–180 are included in the marine air masses group. The seasonal mean O_3 and CO concentrations in marine and continental-polluted air masses along with the percentage frequency of air masses in each group are shown in Table 3. During winter season, winds dominantly originated from continental regions (95 %) and very few arrived from marine regions (5 %). This was an incident with a higher seasonal average of O_3 and CO concentrations from continental air masses as compared to that of marine origin. Hence, a high continental influence (estimated as a difference of average values in continental-polluted and marine air masses) on O_3 (~20 ppbv) and CO (~121 ppbv) was observed in this season. During the pre-monsoon season, only 37 %

Table 2 Surface O_3 concentrations measured at various Indian locations

Sl. no.	Stations	Values	Location	Period	Remarks	Reference
1.	Trivandrum (8.55° N, 77° E)	40 ppb	Coastal	2008–2009	Winter maximum	David and Nair 2011
2.	Central Bay of Bengal (10–15° N, 84–86° E)	60–64 ppb	Oceanic	During 18th Feb–23rd March	Ship measurements	Lal et al. 2006
3	Tranquebar (11° N, 79.9° E)	23±9 ppb	Coastal	1997–2000	Maximum summer	Debaje et al. 2003
4.	Kannur (11.9° N, 75.4° E)	44±3.1 ppbv	Coastal	2009–2010	Maximum winter	Nishanth et al. 2012
5.	Chennai (13.04° N, 80.23° E)	23±14 ppbv	Highly populated urban area	May 2005	Summer high	Pulikesi et al. 2006
6.	Gadanki (13.5° N, 79.2° E),	~16–36 ppbv	Rural site	1993–1996	Maximum value winter to spring	Naja and Lal 2002
7.	Anantpur (14.62° N, 77.65° E)	56.1±9.9 ppb	Semi-arid rural site	Maximum value (April 2010)	Summer high	Reddy et al. 2012
8.	TIFR-NBF (17.47 °N, 78.58° E) Hyderabad	56±14 ppb	Semi-arid urban site	Maximum seasonal (summer 2010)	Summer maximum	Swamy et al. 2012
9.	Pune (18.54° N, 73.81° E)	43.02±16.47 ppbv	Tropical semi-urban site	2003–2004	Summer high	Beig et al. 2007
10.	Bhubaneswar (20°30′ N, 85°83′ E)	Winter (DJF) (50.61±11.28 ppbv)	Coastal	2010 Dec–2012 Nov	Winter high	Present Study
11.	Kolkata (22.36° N, 88.24° E)	5–65 ppb	Urban polluted	June 2003–May 2004	Maximum during autumn and winter	Purkait et al. 2009
12.	Ahmedabad (23° N, 72.6° E)	Autumn 25.1±18.1 Winter 24.4±15.3 ppbv	Urban	1991–1995	Higher O_3 during autumn and winter months	Lal et al. 2000
13.	Mount Abu (24.6° N, 72.7° E)	46 ppbv	High altitude	Monthly avg between 1993 and 200	Maximum winter	Naja et al. 2003
14.	Hissar (25.5′ N, 74.46′ E)	33.4±9.6	Semi-urban site	(Clear days) December 2004	1-month measurement	Lal et al. 2008
15.	Varanasi (25°78′ N, 83°1′ E)	45.18 to 62.35 ppbv	Gangetic Plains	2002–2006	Summer maximum (March–June)	Tiwari et al. 2008
16.	Dibrugarh (27.4° N, 94.9° E)	24±8 (Apr–May)	Semi-urban	November 2009 to May 2013	Summer maximum	Bhuyan et al. 2014
17.	Agra (27°10′ N, 78°05′ E)	Summer (MAMJ) 42–45 ppbv Winters (NDJF) 28–30 ppbv	Suburban site with no industrial activity	Nov 2008–Oct 2009	Summer high	Singla et al. 2011
18.	NPL-New Delhi (28.65′ N, 77.27′ E)	62–95 ppb Summer (AMJ) 50–82 ppb Autum (ON)	Urban	1997–2003	Avg maximum summer	Jain et al. 2005
19.	Pantnagar (29.0° N, 79.5° E)	39±18.9 ppb	IGP	(March 2009–June 2011)	Spring maximum	Ojha et al. 2012
20.	ARIES Nainital (29.37° N, 79.45° E)	67.2±14.2 ppbv	High altitude	Late spring (May 2007)	Spring high	Kumar et al. 2010
21.	Mohal, Kullu (31.9° N, 77.12° E)	75.9±10.12 ppbv in May 2010	Semi-urban site	2010	Summer maximum	Sharma et al. 2013

Table 3 Seasonal average values of O_3 (ppbv) and CO (ppbv) classified by transport pathways along with percentage frequency of winds

	O_3 continental	O_3 marine	O_3[a]	CO continental	CO marine	CO[a]	Continental % frequency	Marine % frequency
Winter	61.67±12.77	42.09±19.31	19.58	399.36±96.45	277.87±76.73	121.48	94.48	5.52
Pre-monsoon	52.31±16.06	44.88±14.75	7.42	317.40±57.08	289.90±50.26	27.49	37.23	62.77
Monsoon	34.34±7.52	33.12±7.79	1.21	209.81±47.85	220.20±43.60	−10.38	59.83	40.17
Post-monsoon	41.77±11.12	25.87±4.34	15.90	293.15±65.39	218.84±39.72	74.30	94.43	5.57

[a] Difference between continental and marine

frequency of air masses came from the continental origin, whereas 63 % was from marine origin. It may be noted that this estimated frequency of air mass arrival during pre-monsoon season is affected strongly by absence of

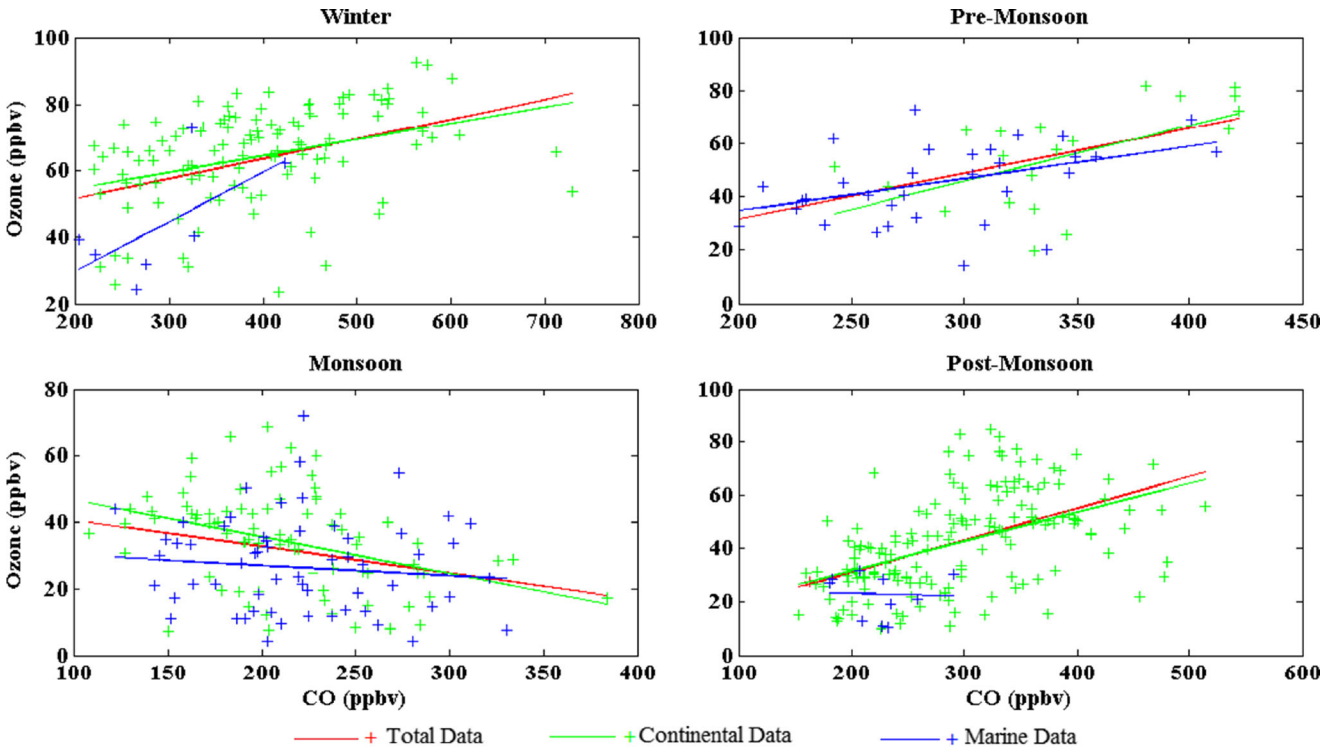

Seasons	Origin	R^2	Slope	Intercept
Winter	Marine	0.41	0.15	-0.49
	Continental	0.15	0.05	44.31
	Total	0.19	0.06	39.42
Pre-monsoon	Marine	0.18	0.12	10.78
	Continental	0.35	0.21	-17.21
	Total	0.31	0.17	-2.22
Monsoon	Marine	0.007	-0.03	32.93
	Continental	0.14	-0.11	57.48
	Total	0.07	-0.08	48.62
Post-monsoon	Marine	0.003	-0.01	25.33
	Continental	0.24	0.11	9.70
	Total	0.26	0.12	7.08

Fig. 5 **a** Winter, **b** pre-monsoon, **c** monsoon, and **d** post-monsoon O_3 and CO correlation curves for all the data points available for each season in both the years

measurements during March–April. Average CO values of continental air mass are estimated to be slightly higher during pre-monsoon than monsoon. In case of O_3, also continental average O_3 was slightly more than that of marine origin. The continental high might be due to photochemical production that is dominant during this season. In case of monsoon season, 60 % frequency of winds originated from continental areas, whereas only 40 % came from marine sources. However, there was hardly any difference between O_3 and CO concentrations coming from different sources. This resulted in no continental influence in case of O_3 and a slightly negative continental influence in case of CO. This could be due to the washout effect and decreased photochemical activity associated with increased cloud cover in this season of the year. During the post-monsoon season, the wind pattern change from onshore to offshore and 94 % frequency of winds were from continental origin, whereas only 6 % came from marine region. This resulted in a gradual build up of average O_3 and CO from continental origin (~42 and ~293 ppbv, respectively) in comparison to marine sources (~26 and ~219 ppbv, respectively). Thus, the net continental influence on O_3 (~16 ppbv) and CO (~74 ppbv) starts to increase during post-monsoon season.

Relationship between O_3 and CO

Seasonal daytime daily averages for O_3 and CO were used for the whole study period of 2 years (Dec 2010 to Nov 2012) to determine the correlation between the entire, continental, and marine data sets of CO and O_3 (Fig. 5). The study suggests the following:

Winter marine During winter, very few air masses originate from a marine location which travels through continental parts (where two major ports and a couple of fertilizer industries are located) before reaching the observation site. This pathway is likely to incorporate a certain amount of CO into the air mass, and therefore, a positive correlation between CO and O_3 is observed; however, the R^2 value of 0.41 is due to availability of fewer data points.

Winter continental The correlation between CO and O_3 is less significant (R^2=0.15) compared to marine, and at the same time, the slope is less stiff. From this observation, it can be inferred that the effect of CO as a precursor during winter is much less. However, a positive value of the *y*-intercept (44.31) indicates that O_3 concentration is significant even when CO concentration is negligible. This typical observation is an indication that during winter, the continental air mass might

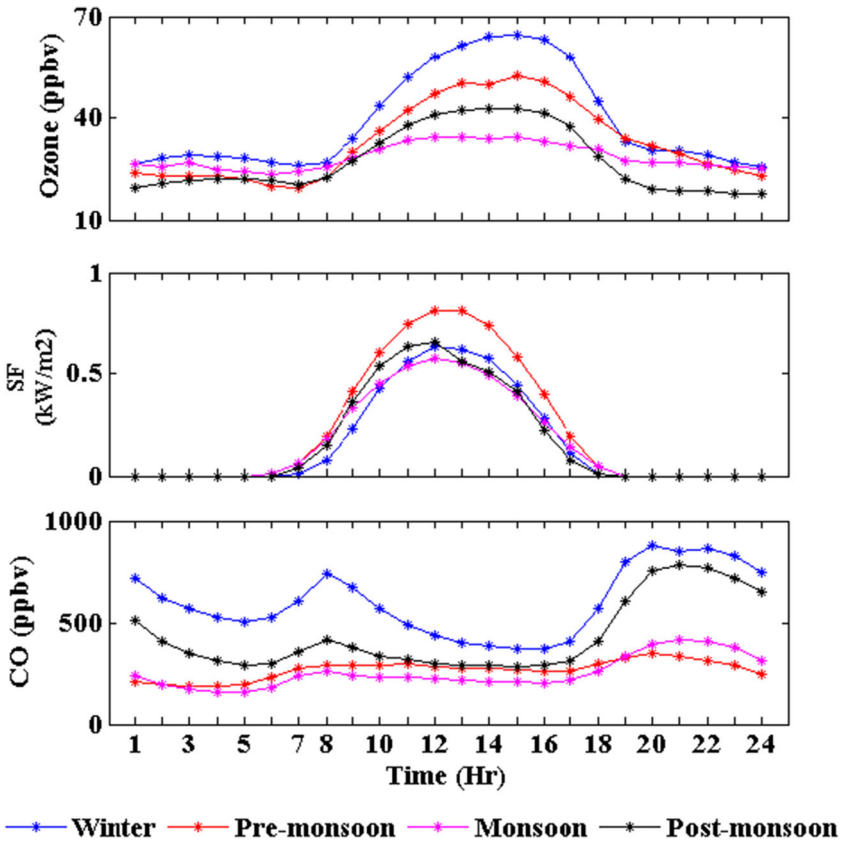

Fig. 6 Seasonal average diurnal variation of O_3, CO, and solar flux (SF) during December 2010 to November 2012

also carry other O_3 precursors to the site leading to a significant rise of the latter.

Pre-monsoon marine A positive correlation is observed between O_3 and CO; however, the R^2 (0.18) is not very significant. This shows that though CO could be one of the precursors that facilitate surface O_3 formation, however, it may not be the dominant one.

Pre-monsoon continental The correlation between CO and O_3 is significant (R^2=0.35) compared to all other seasons, and simultaneously, the slope is also stiffer (0.21); however, a negative *y*-intercept indicates that the role of CO is dominant as a precursor.

Monsoon-marine During this period, no co-relationship was established between CO and O_3 (R^2=0.007).

Monsoon-continental During the same season, continental effect between CO and O_3 is somewhat visible (R^2=0.14), while the negative slope indicates lowering of surface O_3 concentration due to an impediment in photochemical activity as a result of cloud cover and frequent rain showers. It could further be stated that CO, being a primary pollutant, emission is a continual process, though the concentration of the same during monsoon is lower in comparison to other seasons due to washout effects.

Post-monsoon marine No particular correlation (R^2=0.003) between CO and O_3 was observed during this period.

Post-monsoon continental The continental effect is significant between CO and O_3 (R^2=0.24), and from the positive slope, it can be inferred that an increase in CO concentration has a positive impact on surface O_3 concentration.

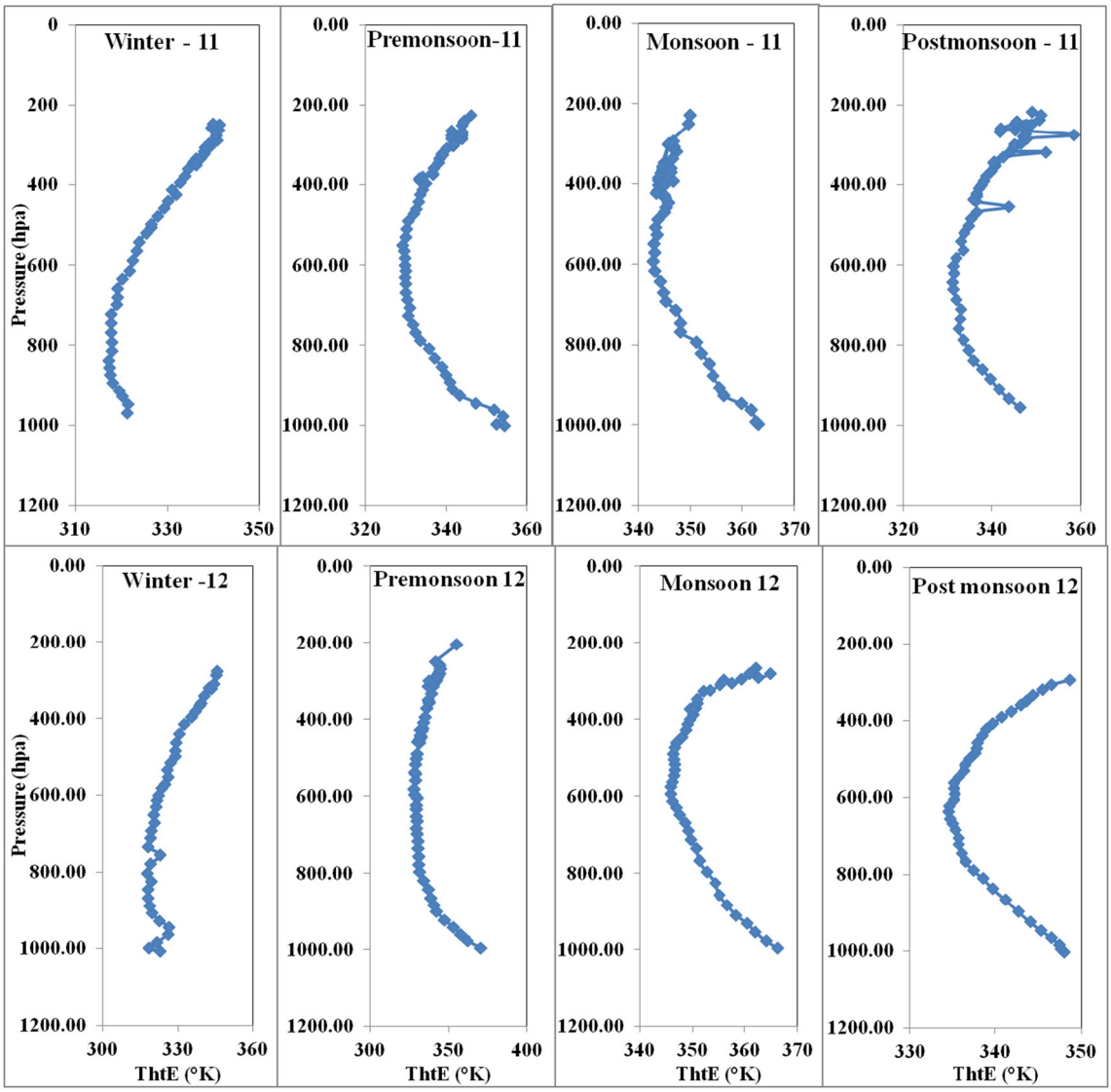

Fig. 7 Seasonal variation of equivalent potential temperature vs pressure at 0000 GMT during December 2010 to November 2012

Diurnal variation in O_3 and CO

Diurnal variation of O_3 shows a typical daytime high with a peak in the afternoon coinciding with the peak in solar flux and slowly decreases with the decrease of later during the evening (Fig. 6). O_3 starts building up at around 0800 h local time during winter and 0700 h local time during pre-monsoon while reaching its peak during the noon (1100–1400 h). O_3 concentration remains more or less steady until 1600–1700 h and then starts decreasing until it reaches a minimum value during midnight. O_3 formation, being a photochemical reaction, represents a daytime high throughout the measurement period in comparison to night (David and Nair 2011). However, during the monsoon season, the diurnal curve is not as pronounced as the other seasons, particularly during the daytime, which might be due to the impact of cloud cover restricting the penetration of solar radiation as well as washout of precursors due to rainfall. The diurnal variation of CO follows a bimodal peak distribution depicting a daytime low, showing a peak during the early morning and other peak during late evenings (Fig. 6). The nighttime high has been linked with the boundary layer activity and meteorological conditions that prevailed over this region. This diurnal variation of CO (low during daytime) and O_3 (higher during the daytime) indicates the role of CO as an O_3 precursor (Henne et al. 2008). In addition, deeper boundary layer during the daytime also leads to mixing of CO emissions into a larger volume and contribute to daytime low in CO mixing ratios.

To determine the role of boundary layer meteorology during various seasons, upper air data for Bhubaneswar were obtained from the University of Wyoming's website (http://weather.uwyo.edu/upperair/) at 0000 GMT (0530 IST) on a daily basis. Daily profiles for all available data in a season were averaged to generate the seasonal average profiles. Analysis has been done taking into account the thermodynamic variables such as equivalent potential temperature (θ_e/ThtE) and pressure. A minimum θ_e value has been used to identify a characteristic feature of inversion (Mallik et al. 2012) and is also considered to be better than normal temperature as it is normalized with respect to pressure and moisture.

Figure 7 shows the inversion condition at different pressure levels in four different seasons during December 2010 to November 2012. Winter season indicates a close association between pollution concentration and boundary layer variation. Inversion, characterized by a minimum in θ_e value, is corresponding to a pressure level of ~900 hPa and indicates a very low mixing height. A lower mixing height prevents the escape of pollutants into the upper atmosphere, resulting in confinement leading to the accumulation of pollutants near the surface. This could also be one of the prime reasons for higher concentration of O_3 precursors like CO which ultimately results in a higher potential for surface O_3 formation. In the pre-monsoon, the inversion was observed to be much deeper, suggesting an increase in mixing height that enhances the dilution of pollutants thereby reducing their concentration near the surface. This might even be the fact for higher concentration of CO during winters than in other seasons. However, during monsoon, this variation was not very clear probably due to unstable atmospheric conditions and ongoing monsoonal circulations.

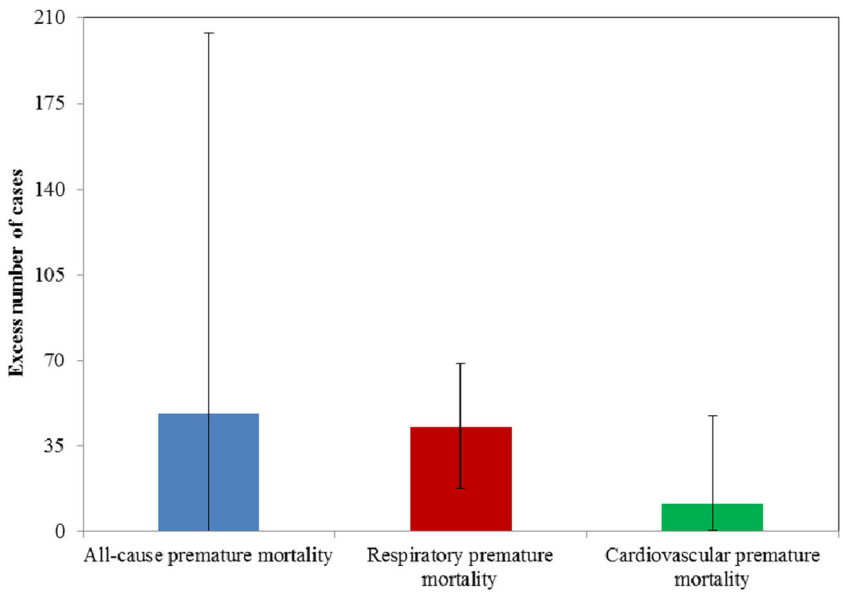

Fig. 8 Health effects of O_3 (with high and low range) during study period (December 2010 and November 2012)

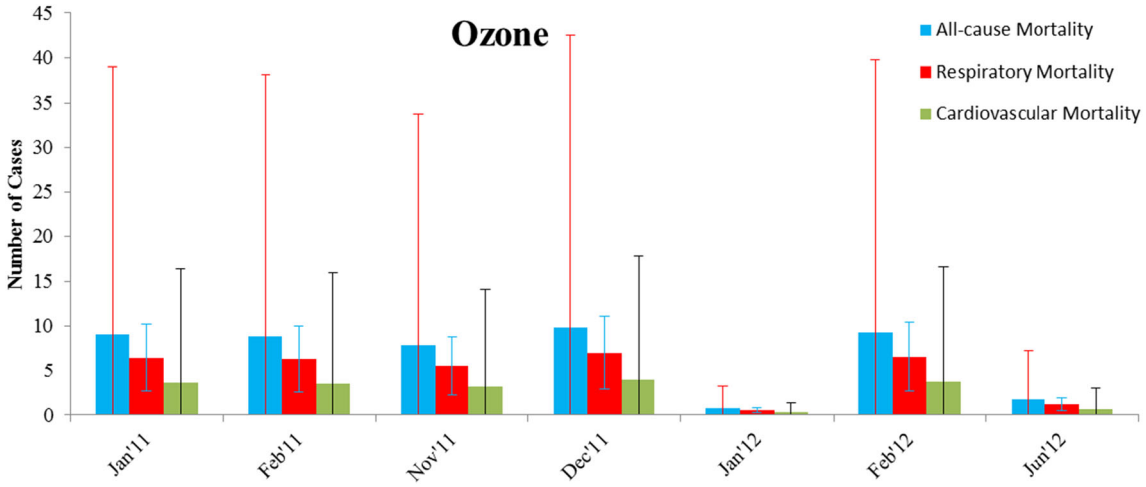

Fig. 9 Monthly distribution of O_3-related health effects from December 2010 to November 2012

Total health effects during study period

Although we have estimated health risks in terms of premature mortality due to exposure of the adult population to CO and O_3, results pertaining to CO are not shown because the ambient air CO concentrations do not exceed the WHO guidelines. Figure 8 illustrates estimated health effects during the entire study period (December 2010 to November 2012) for adults (age 16–59 years) associated with exclusive change in ambient O_3 concentrations. It is estimated that during the study period of December 2010 to November 2012, the ambient O_3 concentrations are responsible for 48 cases of total premature mortality in adults. Further, as shown in Fig. 8, CRF for cardiovascular mortality associated with ambient O_3 concentration is only 16 % of respiratory mortality and thus results in less number of cardiovascular mortality cases.

Figure 9 shows the monthly distribution of estimated health effects during the study period (December 2010 to November 2012) for adults (age 16–59 years) associated with changes in ambient O_3 concentrations. Health effects (premature mortality cases) peaks are observed in winter season (December, January, February) as a result of significantly higher concentrations of ambient O_3 during winter.

There is scarcity of such studies on air pollution-induced health risk estimates for Indian cities. Nevertheless, Lelieveld et al. (2013) adopted concentration response functions derived from western countries and estimated 3,188 cases of respiratory premature mortality associated with O_3 for the highly polluted Indian city, Delhi. On the contrary, the health effects estimated in our study are based on concentration response functions derived from a meta-analysis study conducted in the Asian subcontinent. Also, Bhubaneswar is a smaller and cleaner city in comparison to Delhi, which is reflected in less cases of respiratory premature mortality in case of Bhubaneswar.

Conclusion

In this study, ground-based measurements of O_3 and CO carried out at Bhubaneswar (an urban coastal location situated on the east coast of India) during December 2010 to November 2012 are presented. The daytime O_3 mixing ratio is found to be higher during winter and pre-monsoon (winter being higher than pre-monsoon) followed by post-monsoon and least during monsoon. Various meteorological conditions such as calm weather, lower wind speed, and shallow boundary layer accompanied with the long-range transport of pollutants (which carry precursor gases) are likely to be the cause of winter high. Whereas, a comparatively low surface O_3 concentration in pre-monsoon might be due to vertical mixing of trace gases due to very high temperature conditions (convective activity), higher wind speed, expanded boundary layer conditions, frequent high wind, shower events (Kal Bhairavi), and travel of air masses from cleaner regions (maritime air mass). Similarly, CO was also found to be highest during winter season likely due to higher regional emissions. Diurnal variations show a daytime high in O_3 and a low in CO which are typical of urban sites. Frequency of continental air mass were found to be more during winter in comparison to the marine air mass further supporting the role of long-range transport of precursor trace gases during winter.

Based on ambient air concentrations of CO and O_3, health risk estimates have been made using concentration response functions (CRFs). The health risk estimates show that during

the study period of December 2010 to November 2012, the ambient O_3 concentrations are responsible for 48 cases of total premature mortality in adults. However, comparatively low CO concentrations in the study area do not result in any health effects even in winter.

Acknowledgments The authors are thankful to the Director, Institute of Minerals and Materials Technology (CSIR-IMMT) and the Head, Environment and Sustainability Department (CSIR-IMMT) for their encouragement. Financial support by the ISRO-GBP-ATCTM as well as CSIR is gratefully acknowledged. Analyses and visualizations used in this study were produced by the Giovanni online data system, developed and maintained by the NASA GES DISC. Use of data from ECCAD database is also acknowledged. The authors acknowledge the Director IMD-Bhubaneswar for providing meteorological data. The authors would like to acknowledge Mr. Chinmay Mallik for fruitful discussions, Rajesh and Milan for arrangement of the voluminous data.

References

Atkinson RW, Cohen A, Meheta S, Anderson HR (2011) Systematic review and meta-analysis of epidemiological time-series studies on outdoor air pollution and health in Asia. Air Qual Atmos Health 5(4):383–391

Aubard Y, Magne I (2000) Carbon monoxide poisoning in pregnancy. BJOG: An Int J Obstet Gynaecol 107(7):833–838

Beig G, Gunthe S, Jadhav DB (2007) Simultaneous measurements of O_3 and its precursors on a diurnal scale at a semi urban site in India. J Atmos Chem 57:239–253

Bhuyan PK, Bharali C, Pathak B, Kalita G (2014) The role of precursor gases and meteorology on temporal evolution of O_3 at a tropical location in northeast India. Environ Sci Pollut Res. doi:10.1007/s11356-014-2587-3

Cao J, Yang C, Li J, Chen R, Chen B, Gu D, Kan H (2011) Association between long-term exposure to outdoor air pollution and mortality in China: a cohort study. J Hazard Mater 186(2–3):1594–1600

Cohen A (2005) The global burden of disease due to outdoor air pollution. J Toxicol Env Heal A68(13–14):1301–1307

Cropper M, Gamkar S, Malick K, Limonov A, Partridge I (2012) The health effects of coal electricity generation in India. Discussion Paper RFF DP 12–25, 1616 P St. NW Washington, DC 20036

Crutzen PJ (1973) A discussion of the chemistry of some minor constituents in the stratosphere and troposphere. Pure Appl Geo-Phys 106–108:1385–1399

David LM, Nair PR (2011) Diurnal and seasonal Variability of surface O_3 and NOx at a tropical coastal site: association with mesoscale and synoptic meteorological conditions. J Geophys Res 116, D10303

Debaje SB, Jeyakumar SJ, Ganesan K, Jadhav DB, Seetaramayya P (2003) Surface O_3 measurements at tropical rural coastal station Tranquebar, India. Atmos Environ 37:4911–4916

Desqueyroux H, Pujet JC, Prosper M, Moullec YL, Momas I (2002) Effects of air pollution on adults with chronic obstructive pulmonary disease. Arch Environ Health: Int J 57(6):554–560

Fishman J, Seller W (1983) Correlative nature of O_3 and carbon monoxide in the troposphere' implications for the tropospheric O_3 budget. J Geophys Res-Oceans 88(C6):3662–3670

Granier C, Bessagnet B et al (2011) Evolution of anthropogenic and biomass burning emissions of air pollutants at global and regional scales during the 1980–2010 period. Clim Chang 109(1–2):163–190

Gurjar BR, Jain A, Sharma A, Agrawal A, Gupta P, Nagpure AS, Lelieveld J (2010) Human health risks in megacities due to air pollution. Atmos Environ 44(36):4606–4613

Guttikunda SK, Goel R (2012) Health impacts of particulate pollution in a Megacity Delhi, India. Environ Dev 6:8–20

HEI (2004) Health effects of outdoor air pollution in developing countries of Asia: a literature review. Special Report 15, Health Effects Institute, Boston

HEI (2010) Outdoor air pollution and health in the developing countries of Asia: a comprehensive review, Special Report 18. Health Effects Institute, Boston

HEI (2011) Public Health and Air Pollution in Asia (PAPA): coordinated studies of short-term exposure to air pollution and daily mortality in two Indian cities. Research Report 157. Health Effects Institute, Boston

Henne S, Klausen J, Junkermann W, Kariuki JM, Aseyo JO, Buchmann B (2008) Representativeness and climatology of carbon monoxide and O_3 at the global GAW station Mt. Kenya in equatorial Africa. Atmos Chem Phys 8:3119–3139

Jain SL, Arya BC, Kumar A, Ghude SD, Kulkarni PS (2005) Observational study of surface O_3 at New Delhi, India. Int J Remote Sens 26(16):3515–3524

Kalita G, Bhuyan PK (2011) Spatial heterogeneity in tropospheric column O_3 over the Indian subcontinent: long-term climatology and possible association with natural and anthropogenic activities. Advances in Meteorology Article ID 924516. doi:10.1155/2011/924516

Kandlikar M, Ramachandran G (2000) The causes and consequences of particulate air pollution in urban India: a synthesis of the science. Annu Rev Env Resour 25:629–684

Khalil MAK, Rasmussen RA (1990) The global cycle of carbon monoxide: trends and mass balance. Chemosphere 20(1–2):227–242

Kumar R, Naja M, Venkataramani S, Wild O (2010) Variations in surface O_3 at Nainital: a high altitude site in the central Himalayas. J Geophys Res 115(D):16302

Kumar R, Naja M, Pfister GG, Barth MC, Brasseur GP (2013) Source attribution of carbon monoxide in India and surrounding regions during wintertime. J Geophys Res-Atmos 118:1981–1995

Kurokawa J, Ohara T, Morikawa T et al (2013) Emissions of air pollutants and greenhouse gases over Asian regions during 2000–2008: Regional Emission inventory in ASia (REAS) version 2. Atmos Chem Phys 13:11019–11058

Lal S, Naja M, Subbaraya BH (2000) Seasonal variations in surface O3 and its precursors over an urban site in India. Atmos Environ 34: 2713–2724

Lal S, Chand D, Sahu LK, Venkatramani S, Brasseur G, Schultz MG (2006) High levels of O3 and related gases over the Bay of Bengal during winter and early spring of 2001. Atmos Environ 40:1633–1644

Lal S, Sahu LK, Gupta S, Srivastava S, Modh KS, Venkataramani S, Rajesh TA (2008) Emission characteristic of O3 related trace gases at a semi-urban site in the Indo-Gangetic plain using intercorrelations. J Atmos Chem 60:189–204

Lawrence MG, Lelieveld J (2010) Atmospheric pollutant outflow from southern Asia: a review. Atmos Chem Phys 10:11017–11096

Lelieveld J, Barlas C, Giannadaki D, Pozzer A (2013) Model calculated global, regional and megacity premature mortality due to air pollution. Atmos Chem Phys 13(14):7023–7037

Levine JS (1996) Biomass burning and global change. In: Remote sensing, modelling and inventory development, and biomass burning in Africa. MIT, Cambridge

Lin YC, Lin CY, Lin PH, Engling G, Kuo TH, Hsu WT, Ting CC (2011) Observation of O3 and carbon monoxide at Mei-Feng mountain site (2269 m a.s.l.) in Central Taiwan: seasonal variations and influence of Asian continental outflow. Sci Total Environ 409:3033–3042

Lvovsky K, Hughes G, Maddison D, Ostro B, Pearce D (2000) Environmental cost of fossil fuels: a rapid assessment methods with application to six cities. The World Bank,78

Mahapatra PS, Jena J, Moharana S, Srichandan H, Das T, Roy Chaudhury G, Das SN (2012) Surface O3 variation at Bhubaneswar and intra-correlationship study with various parameters. J Earth Syst Sci 121: 1163–1175

Mallik C, Venkataramani S, Lal S (2012) Study of a high SO_2 event observed over an urban site in western India. Asia-Pac J Atmos Sci 48(2):171–180

Mauzerall DM, Wang X (2001) Protecting agricultural crops from the effects of tropospheric O3 exposure: reconciling science and standard setting in the United States, Europe and Asia. Annu Rev Energy Environ 26:237–268

Naja M, Lal S (2002) Surface O3 and precursor gases at Gadanki (13.5_N, 79.2_E), a tropical rural site in India. J Geophys Res 107(D14):4197

Naja M, Lal S, Chand D (2003) Diurnal and seasonal variabilities in surface O3 at a high altitude site Mt Abu (24.6_N, 72.7_E, 1680 m asl) in India. Atmos Environ 37:4205–4215

Nishanth T, Sateesh Kumar MK, Valsaraj KT (2012) Variation in surface O3 and NOx at Kannur: a tropical coastal site in India. J Atmos Chem 69:101–126

Ohara T, Akimoto H et al (2007) An Asian emission inventory of anthropogenic emission sources for the period 1980–2020. Atmos Chem Phys 7:4419–4444

Ojha N, Naja M, Singh KP, Sarangi T, Kumar R, Lal S, Lawrence MG, Butler TM (2012) Variabilities in O3 at a semi-urban site in the Indo-Gangetic Plain region: association with the meteorology and regional processes. J Geophys Res 117, D20301

Olivier JGJ, Bloos JPJ, Berdowski JJM, Visschedijk AJH, Bouwman AF (1999) A 1990 global emission inventory of anthropogenic sources of carbon monoxide on 1°×1° developed in the framework of EDGAR/GEIA. Chemosphere Global Change Sci 1:1–17

Ostro B (1994) Estimating the health effects of air pollutants: a method with an application to Jakarta, policy research working paper No. 1301. World Bank, Washington, DC

Patankar AM, Trivedi PL (2011) Monetary burden of health impacts of air pollution in Mumbai, India: implications for public health policy. Public Health 125:157–164

Penney S, Bell J, Balbus J (2009) Estimating the health impacts of coal-fired power plants receiving international financing. Environmental Defense Fund, NW, Washington, DC

Pope CA, Burnett RT, Thun MJ, Calle EE, Krewski D, Ito K, Thurston GD (2002) Lung cancer, cardiopulmonary mortality, and long-term exposure to fine particulate air pollution. JAMA-J Am Med Assoc 287(9):1132–1141

Pulikesi M, Baskaralingam P, Rayudu VN, Elango D, Ramamurthi V, Sivanesan S (2006) Surface O3 measurements at urban coastal site Chennai, in India. J Hazard Mater B137:1554–1559

Purkait NN, De S, Sen S, Chakrabarty DK (2009) Surface O3 and its precursors at two sites in the north east coast of India. Indian J Radio Space Phys 38:86–97

Reddy RR, Ram Gopal K et al (2008) Surface O3 measurements at Anantapur (AP) India. Indian J Radio Space Phys 37:209–215

Reddy BSK, Kumar KR, Balakrishnaiah G et al (2012) Analysis of diurnal and seasonal behavior of surface O3 and its precursor (NOx) at a semi-arid rural site in southern India. Aerosol Air Qual Res 12:1081–1094

RGI (2012a) Sample registration system, statistical report, 2010, SRS analytical studies, report number 1 of 2012, Office of the Registrar General, India, Government of India. Ministry of Home Affairs, 2A, New Delhi

RGI (2012b) Report on medical certification of cause of death, Office of the Registrar General, India, Government of India. Ministry of Home Affairs, 2A, New Delhi

Sharma P, Kuniyal JC, Chand K, Guleria RP, Dhyani PP, Chauhan C (2013) Surface O3 concentration and its behaviour with aerosols in the northwestern Himalaya, India. Atmos Environ 71: 44–53

Sikder HA, Suthawaree J, Kato S, Kajii Y (2011) Surface O3 and carbon monoxide levels observed at Oki, Japan: regional air pollution trends in East Asia. J Environ Manag 92:953–959

Silva RA, West JJ, Zhang Y, Anenberg SC et al (2013) Global premature mortality due to anthropogenic outdoor air pollution and the contribution of past climate change. Environ Res Lett 8(3):034005

Singla V, Satsangi A, Pachauri T, Lakhani A, MaharajKumari K (2011) O3 formation and destruction at a sub-urban site in North Central region of India. Atmos Res 101:373–385

Sudo K, Akimoto H (2007) Global source attribution of tropospheric O3: long-range transport from various source regions. J Geophys Res: Atmos 112:D12,27

Swamy YV, Nikhil GN, Venkanna R, Dhulipala NSKC, Sinha PR, SrinavasanS AGR (2012) Role of nitrogen oxides, black carbon, and meteorological parameters on the variation of surface O3 levels at a tropical urban site—Hyderabad, India. CLEAN – Soil Air Water 41(3):215–225

Tiwari S, Rai R, Agrawal M (2008) Annual and seasonal variations in tropospheric O3 concentrations around Varanasi. Int J Remote Sens 29(15):4499–4514

WHO (2006) WHO air quality guidelines for particulate matter, O3, nitrogen dioxide and sulfur dioxide, global update 2005, summary of risk assessment, WHO/SDE/PHE/OEH/06.02. World Health Organization, Geneva